Available online at www.eccomasproceedia.org
Eccomas Proceedia COMPDYN (2021) 3957-3969

ECCOMAS
Proceedia

COMPDYN 2021
8th ECCOMAS Thematic Conference on
Computational Methods in Structural Dynamics and Earthquake Engineering
M. Papadrakakis, M. Fragiadakis (eds.)
Streamed from Athens, Greece, 28 - 30 June 2021

SEISMIC PERFORMANCE OF STEEL MRFs RETROFITTED WITH BRBS: INFLUENCE OF THE DESIGN DECISIONS FOR THE DEVICES

Fernando Gutiérrez-Urzúa[1] **and Fabio Freddi**[1]

[1] Dept. of Civil, Environmental & Geomatic Engineering, University College London
Gower St., London, WC1E 6BT, U.K.
{f.urzua,f.freddi}@ucl.ac.uk

Abstract

Buckling Restrained Braces (BRBs) represent an effective strategy for the seismic retrofit of existing steel Moment Resisting Frames (MRFs), as they contribute to increase the strength, stiffness and energy dissipation capacity of the frame. Nonetheless, the design choices made during the retrofit process have a significant impact on the performance of the structure. For example, the inclusion of 'large' BRBs (i.e., high yielding strength and stiffness) may contribute to limit the deformation demands in the MRF; nonetheless, it may also induce large forces in the beams and columns of the existing structure. On the other hand, the inclusion of 'smaller' BRBs (i.e., low yielding force and stiffness), while allowing reaching the required safety requirements, may not be able to protect the MRF from damage. Additionally, the sizing of the BRB elements has an influence on the seismic demand parameters affecting the global performance of structural and non-structural components (i.e., peak and residual drifts, as well as storey accelerations). The present study investigates the impact of the design choices in the seismic performance of a retrofitted three-storey case-study frame by considering three retrofit options. The case-study MRF for the bare frame and the three retrofit configurations are modelled and numerically investigated in Opensees by monitoring local damage states (e.g., damage in BRBs, beams, columns, panel zones). First, a comparison is made in terms of non-linear static analyses to identify the deficiencies of the structures. Then, a fragility analysis is carried out through Incremental Dynamic Analyses (IDAs) accounting for the influence of the record-to-record variability. Finally, a comparison is made in terms of local and global Engineering Demand Parameters, by developing fragility curves for the components, for storey drifts and accelerations.

Keywords: Buckling-restrained braces; Seismic retrofit; Design strategy; Local engineering demand parameters; Fragility curves.

ISSN:2623-3347
Peer-review under responsibility of the organizing committee of COMPDYN 2021.
doi: 10.7712/120121.8759.18979

1 INTRODUCTION

Buckling Restrained Braces (BRBs) have proven to be effective in improving the seismic performance of existing and new Moment Resisting Frames (MRFs) [1–3]. Such devices can be included within diagonal steel bracing connected to the existing frame contributing to the strength and stiffness of the existing structures by providing a parallel truss-like force path for the seismic lateral load imposed on the building hence forming a dual system [4]. In addition, the stable hysteretic behaviour provided by the BRBs largely contributes towards the increase of the energy dissipation capacity of the structure [2,5]. Similarly to other yielding devices, BRBs rely on the passive dissipation of elasto-plastic energy through the yielding of a steel core, which is surrounded by an unbonded buckling-restraining sleeve that allows the development of significant compression capacity, thus generating nearly symmetrical hysteretic loops [6,7]. In addition, BRBs require low maintenance and can be easily replaced after a strong earthquake, if required.

Regardless of the multiple advantages of BRBs, several aspects require further investigation. For example, the use of BRBs as a retrofit measure for existing steel MRF is followed by a redistribution of load paths and deformation mechanisms, which may induce larger seismic demands on the existing elements [2]. In addition, while the high ductility of BRBs may provide the structure with large energy dissipation capacity, their low post-yielding stiffness may result in large Residual Inter-storey Drift Ratios (RIDRs) [8], hence jeopardising the operativity and repairability of such structures [9–11]. Besides, residual deformations, together with the device's cumulative damage, may also increase the collapse risk under future earthquakes [12].

When properly designed, the MRF can provide restoring forces to counteract the residual drifts related to the yielding of BRBs [4]. Additionally, the Buckling Restrained Braced Frame (BRBF) can contribute towards the reduction of the floor accelerations arising from higher modes effects [4,13] and can limit the damage in the MRF [8]. Nonetheless, the efficiency of this dual system (*i.e.*, MRF + BRBF) is function of the relative properties of the MRF and the BRBF; therefore, the sizing of the bracing system plays a significant role in the effectiveness of the retrofitting scheme.

The present study aims at evaluating the influence of the design choices in the fragility of steel MRFs retrofitted by means of BRBs. First, the assessment of the un-retrofitted case-study structure is performed by comparing deformation-based local Engineering Demand Parameters (EDPs) (*i.e.,* rotations in beams and columns, distortion in panel zones and ductility demand in the BRBs), with the Acceptance Criteria (AC) corresponding to Performance Levels (PLs) as outlined in the ASCE 41-17 [14]. Successively, the design of three retrofitting schemes is carried out considering different design objectives. Then, the bare and retrofitted structures' seismic response is compared by performing both non-linear static and dynamic analysis in an Incremental Dynamic Analyses (IDAs) [15] fashion. The IDAs are performed considering 30 Ground Motion (GM) records allowing the definition of fragility curves. A few preliminary considerations and insights are provided on the influence of the design objectives in the different parameters characterising the seismic performance of structures retrofitted with BRBs.

2 CASE-STUDY STRUCTURE AND RETROFITTING SCHEMES

The Boston 3-storey, pre-Northridge MRF designed within the SAC Steel Project [16] has been selected for case-study purposes. This structure is representative of low-code pre-Northridge steel MRFs, as it was designed according to the 12th edition of the National Building Code. In this study, the structure is considered to be representative of buildings designed for low seismic demands, which often require retrofitting due to an update in the structural design regulations (*i.e.*, their performance does not comply with new regulations) or those structures

located in regions where design seismic demand was increased as a result of new data on the seismic hazard of the site. The case-study structure was designed assuming stiff soil (Soil Class D in modern standards, *e.g.*, [14,17]), office occupancy, and regular plan distribution and with no considerable irregularities along with the height. In addition, only the perimeter frames are considered to withstand lateral loads (*i.e.*, internal frames are connected as gravity frames only), as it was a common practice in the early 1990s in the United States. Details of the case-study frame are shown in Figure 1.

A 2-D non-linear Finite Element (FE) model of the north-south direction frames is developed in OpenSees [18]. Only this frame is considered in the present study, as the structure is fully symmetric (*i.e.*, torsional effects are negligible). Additional details on the modelling strategy are extensively detailed in Gutiérrez-Urzúa *et al.* [19].

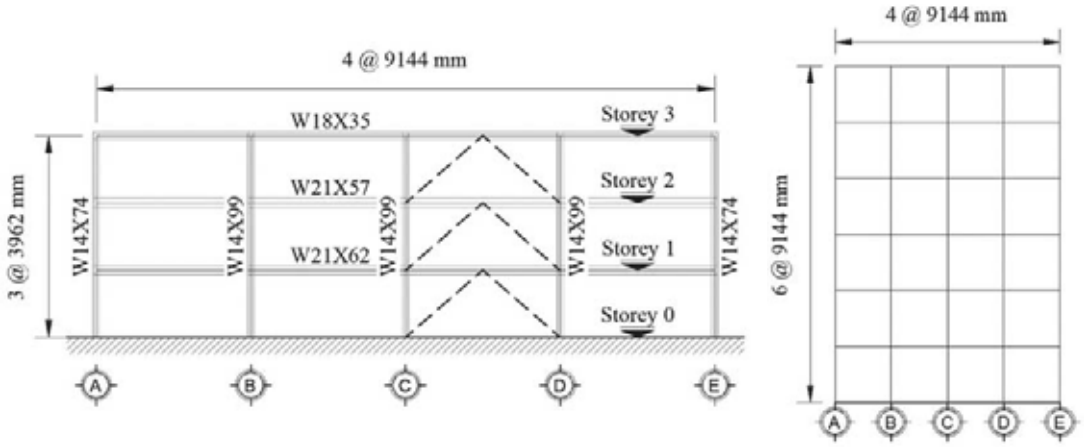

(a) Elevation view **(b) Plan view**

Figure 1: Description of the case-study structure: (a) elevation view of the MRF and location of braces in the retrofitting schemes; (b) plan view of the typical storey floor.

2.1 Assessment of the case-study structure

The first and second periods of vibration are T_1 = 1.88 sec and T_2 = 0.52 sec, which is in agreement with previous studies (*i.e.*, [16]). The mode-shape corresponding to the first mode (*i.e.,* [0.29 0.66 1.00]) shows a relatively uniform distribution of mass and stiffness along with the height. Non-linear static analyses, with lateral loads proportional to the first mode-shape and story mass distribution, are performed to evaluate the local components' capacity hierarchy for each PL and to identify the structure's deficiencies. Figure 2 shows the pushover curves for the Inter-storey Drift Ratios (IDRs), including markers for each local component type (*i.e.,* columns, beams and panel zones), to indicate at which points each AC is overpassed. The PLs and AC used in the present study are those defined in the ASCE 41-17 [14]. The green, yellow and red symbols in Figure 2 are related to the Immediate Occupancy (IO), Life Safety (LS) and Collapse Prevention (CP) PLs, respectively. As observed in Figure 2, the failure of the panel zones (square markers in Figure 2) is the first mechanism to occur at all storeys and PLs. For the IO PL the failure of the panel zones is followed by the columns (circle markers in Figure 2) at the first storey and the beams (triangle markers in Figure 2) at the third storey. The system overpasses the IO PL at a roof drift of 0.11 m (corresponding to IDRs of 0.82%, 1.04% and 0.94% for the first, second and third storeys, respectively). Similarly, the LS and CP PLs are reached simultaneously at a roof drift of 0.44 m (corresponding to IDR of 3.61%, 3.96% and 3.46% for the first, second and third storeys, respectively), as the AC for the panel zones is the same in the LS and CP PLs.

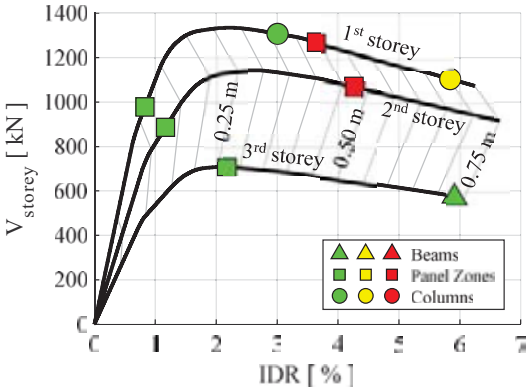

Figure 2: Pushover curves for the un-retrofitted structure. Grey lines relate the IDR at each storey to the roof displacement at every 0.05 m.

2.2 Buckling Restrained Braces (BRBs) retrofitting design

Three retrofit schemes are designed to comply with different design objectives, expressed in terms of target roof displacements (d_u). The first retrofit scheme (R-A) is designed to match the roof displacement at which the first element reaches the CP PL in the MRF structure (panel zones in the first storey, as observed in Figure 2). This represents the design choice where all the resources of the structure are exploited to satisfy the CP requirements. The second retrofit scheme (R-B) is designed based on the roof displacement at which the IDR reaches 2% in any of the storeys, as this is one of the prescribed design limit established by the AISC 341-16 [20] for BRBFs. Finally, the third retrofit scheme (R-C) aims at avoiding damage in the MRF; therefore, the roof displacement is limited to the step at which any of the MRF elements overpasses the IO PL, based on the AC defined by the ASCE 41-17 [14]. Nowadays, there is considerable interest in the definition of seismic-resilient structures (*e.g.,* [11,21,22]) and this third retrofit option aims at limiting the damage to the BRBs only at the CP PL hence allowing an easy and quick repairability of the structure. Table 1 summarises the design limits for the three retrofitting schemes.

Retrofit scheme	Design objective	Target roof displacement, d_u
R-A	Avoid the CP PL in the MRF (according to ASCE 41-17 [14])	0.44 m
R-B	Limiting the IDR to 2% in all storeys (according to AISC 341-16 [20])	0.21 m
R-C	Avoid the IO PL in the MRF (according to ASCE 41-17 [14]	0.11 m

Table 1: Target roof displacements (d_u) for the considered design objectives.

The design process is carried out by considering an equivalent Single-Degree-of-Freedom (SDoF) system approximation [23], based on the bi-linearised (system base shear vs. roof displacement) capacity curves from the original bare frame, with an initial stiffness (k_0) equivalent to the ratio between the 60% of the maximum base shear (F_u), and its corresponding roof displacement. The yielding force and displacement (F_y, d_y) are calculated by considering an equal energy approach (*i.e.*, equal areas under the pushover curves; therefore, defined consistently

with k_0 and d_u), and the equivalent SDoF capacity curves are compared to the seismic demands in the acceleration-displacement response spectrum (ADRS) plane.

The seismic demands are calculated considering Seattle as case-study region (corresponding to a moderate seismic region) and following the approach suggested by the ASCE 41-17 [14]. Seismic Risk Category II and stiff soil (Type D) are considered. All the retrofit schemes are designed by considering the BSE-2E hazard provisions (*i.e.*, 5% probability of exceedance in 50 years); nonetheless, the BSE-2N hazard is also considered, as the code requires to use this hazard level as an upper boundary in those cases in which BSE-2E results in higher demands. The response spectra are built aided by the SEAOC's online tool [24], and further modified to consider a 3% damping ratio (*i.e.*, spectra are multiplied by a factor B_1 for BSE-2E and B_{SSI} for BSE-2N, as specified in ASCE 41-17 [14] and ASCE 7-16 [25], respectively). Figure 3 shows the response spectra for the BSE-2E and BSE-2N hazard levels for the 3% damping ratio. As it can be observed, BSE-2N results in lower demands in all periods; therefore, this spectrum is used for the retrofit design in the present study.

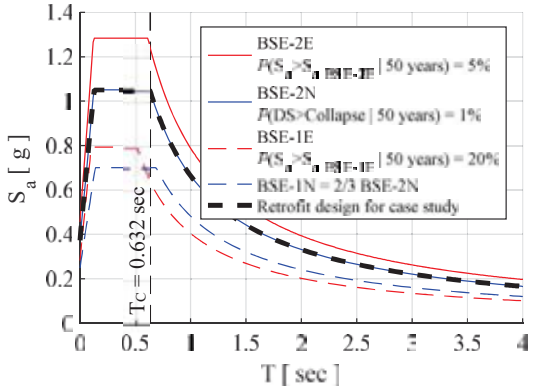

Figure 3: Elastic response spectra for the design of retrofit schemes, corresponding to the BSE-2E and BSE-2N hazard levels. BSE-1E and BSE-1N hazards shown for reference purposes.

Figure 4 shows the comparisons between the seismic demand and capacity for the MRF (*i.e.,* the red lines) by considering the three target roof displacements. The comparison shows the inadequacy of the bare frame and hence the need for retrofitting. At the same time, the figures show the seismic demand and capacity for the retrofitted frames (*i.e.*, the dual system) designed such that the capacity is able to meet the demand (*i.e.,* the blue lines). The retrofitted capacity line is the bilinearised form of the trilinear curve composed by the addition of the MRF capacity line and the BRBF capacity line (*i.e.*, the purple line).The ductility-reduced demands [23] are obtained after bi-linearisation of the systems.

The MRF ductility (μ_{MRF}) is equal to 3.32, 1.74 and 1.17 for the R-A, R-B and R-C schemes, respectively, while the BRBF ductility (μ_{BRBF}) is designed as 18, 14 and 8. The resulting system ductility (μ_{DS}), defined as the ratio between the ultimate and yielding displacements in the dual system bilinearised curve (d_u/d_y), is equal to 4.74, 4.28 and 4.40. In order to match the BRBF stiffness and ductility requirements, the SDoF is de-coupled by considering the original mode shape of the structure, therefore, defining the design requirements at each storey. Finally, the area and length of the BRBs is defined in accordance to the force and ductility requirements for the storey, while the area in the complementing elastic brace is defined in accordance with the stiffness requirements of the storey (*i.e.*, with the elastic brace and BRB working in series). For a more in-depth discussion on the design method, the reader is referred to Freddi *et al.* [26].

The nominal material yield strength (f_y) considered for the BRBs, correspond to steel ASTM A36 (f_y = 248 MPa), which is further increased by 30% for the design, to represent the expected

yield strength (f_{ye}) of the material, based on the ratios provided by the AISC 341-16 [20]. The design ductility (μ_{BRB}) of the BRB material is 20, which is within (and consistent with) the ranges observed in previous experimental work [27]. The elastic braces are made in steel ASTM A500 Grade C (f_y = 317 MPa).

The BRBs are modelled in Opensees [18] by using the *SteelBRB* material [5], while the elastic braces are modelled by considering the *Elastic* material, as they are not expected to yield at any point due to the lower strength in the connected BRBs. Table 2 shows a summary of the BRB properties for each retrofitting scheme.

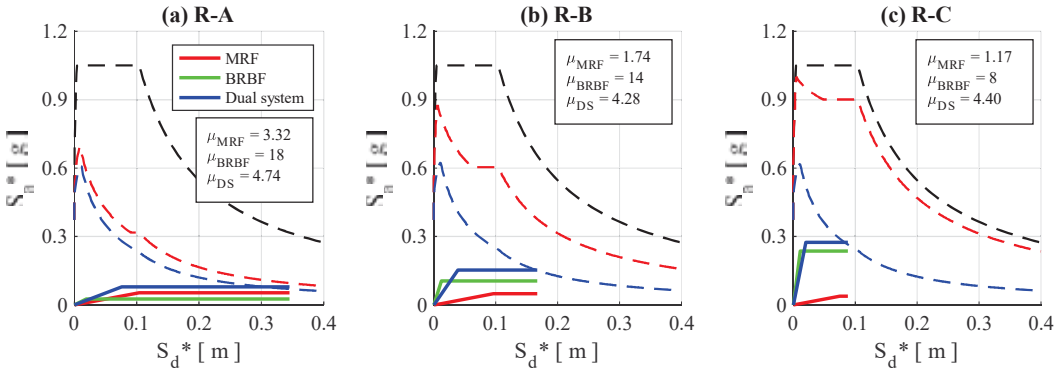

Figure 4: Bi-linearised pushover curves of the equivalent SDoF bare and retrofitted structures, in comparison with the demands, presented in the displacement-acceleration response spectrum (ADRS) plane.

Model	Storey	BRB device		Elastic brace	
		Area [mm^2]	Length [m]	Area [mm^2]	Length [m]
R-A	1	1301	2.96	11542	3.09
	2	1115	3.75	5813	2.30
	3	693	3.47	4385	2.58
R-B	1	5204	1.41	37167	4.64
	2	4460	1.78	23109	4.27
	3	2771	1.08	16017	4.97
R-C	1	11710	0.70	52383	5.35
	2	10034	0.58	34204	5.47
	3	6236	0.54	23280	5.51

Table 2: Characteristics of the BRBs and elastic braces in the different retrofitting schemes.

3 ASSESSMENT OF THE RETROFITTED CASE-STUDY STRUCTURES

After the retrofitting of the case-study building, the structure's fundamental period is reduced from 1.88 s, for the bare frame, to 1.06 s, 0.60 s and 0.50 s for R-A, R-B and R-C, respectively. Non-linear static analyses are performed on the retrofitted structures, and the AC thresholds for all the structural PLs established in ASCE 41-17 [14] are monitored and shown in Figure 5. For BRBs, the AC is expressed in terms of plastic deformations and the CP PL is increased from 13.3 to 19 times the yielding deformation, as this value is consistent with the design ductility of 20.

In the case of R-A, shown in Figure 5a, the structure's improvement allows reaching base shear values over 2000 kN, with PLs that are first overpassed by the BRBs at all storeys. However, the PLs for the panel zones in the IO and CP PLs, closely follows, highlighting the

adequacy of the design strategy in terms of the distribution of the devices stiffness and strength. In addition, when the structure reaches a CP PL, columns in the bottom storey are considered to experience structural damage, as their IO PL is overpassed. In the case of R-B, , shown in Figure 5b, the pushover curves show higher post-yielding stiffness due to the hardening of the BRBs, which provide a larger base shear contribution in this configuration. BRBs control the system failure for all PLs; nonetheless, panel zones reach the IO PL when the BRBs overpass the LS PL, which suggests that the MRF exhibits damage whenever the BRBs overpass this PL. Finally, the case R-C, is shown in Figure 5c. In this case the strength and stiffness contribution of the BRBs is significantly higher, while the BRBs reach the CP LS almost as the panel zones reach the IO LS, which suggests that the MRF remains undamaged while the BRBs reaches its considered failure. It is worth mentioning that the damage scenario observed is consistent with the design objectives which are also represented by the lines for the design displacement d_u (*i.e.,* the blue dotted lines) in Figure 5.

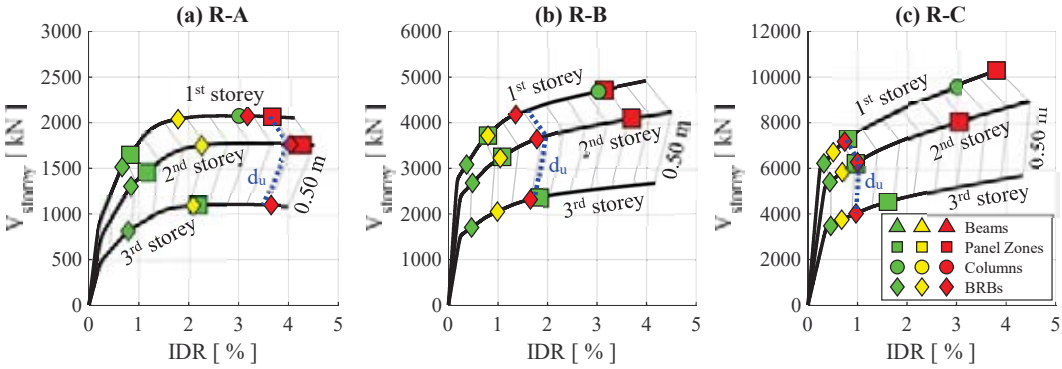

Figure 5: Pushover curves for the retrofitted structures. Grey lines relate the IDR at each storey to the roof displacement at every 0.05 m.

3.1 Fragility of the case-study structure and retrofitting schemes

The fragility of the bare and retrofitted structures is derived based on IDAs [15] by considering a set of 30 GM records selected from the PEER NGA-West2 database [28]. These GMs are selected to be in agreement with the BSE-2N spectrum (see Figure 3), with no further discrimination (all types, with no distinction for distances, wave velocities nor significant duration). Only the acceleration in the *x*-direction is considered.

Based on the results of the IDAs, fragility curves are derived. These provide the probability of the Damage State (DS) exceeding a specific PL in a component (or in the system), conditional to the value of the intensity measure (IM), *i.e.*, $P(\text{DS} \geq \text{PL} \mid \text{IM})$. DSs are defined by the the seismic deformation demands and compared to the capacity (*i.e.*, the element-based AC related to a PL) for all the considered components. The spectral acceleration corresponding to the structure's fundamental period $S_a(T_1)$ is considered as IM [29] in the present study.

The fragility curves for the bare and retrofitted case-study structures are shown in Figure 6. These curves are derived for each element type (*e.g.*, BRBs, columns, beams and panel zones), while the system fragility is defined by considering a series arrangement of the components, *i.e.,* corresponds to the first element (of any kind) to overpass the AC for the considered PL. In addition, fragility curves are built for those cases in which the numerical model does not reach convergence due to excessive deformation (*i.e.*, collapse cases, as defined by Jalayer *et al.*) [30]. Nonetheless, these cases occur once the element-based AC is overpassed in all PLs, therefore, they are simply treated as collapse cases.

Consistently with the observations from the pushover analyses, the panel zones define the system fragility for the bare frame, while the BRBs define the system fragility in the retrofitted cases, *i.e.,* they represent the most fragile components for the whole range of IM values. The direct comparison of fragility curves for the different retrofitting schemes allows to synthetically contrast the capacity of the retrofitting schemes, however, it should be noted that it does not allow to consider the demand changes due to the period shifting, therefore, a comprehensive comparison requires site-dependent hazard considerations.

As it can be observed, the increase of capacity is reflected in the shifting of the fragility curves to higher IM values, accordingly with the retrofitting level. The median intensity values (IM_{50}) of the retrofitted structures are increased by 136%, 255% and 445% for the R-A, R-B and R-C retrofitting schemes for the IO PL; by 54%, 80% and 100% for the LS PL; and by 159%, 184% and 207% for the CP LS. The effect of the record-to-record variability is more noticeable in the retrofitting scheme R-A when compared to R-B and R-C, as reflected by the lognormal standard deviation β values. This effect may be related to the larger ductility of the BRBF in the R-A retrofitting scheme, as highlighted by Freddi *et al.* [4]. It is relevant to highlight that all force-controlled failures (*e.g.*, compression/tension in columns, shear in beams) occur after all the PLs are overpassed, therefore, they do not influence the fragility curves.

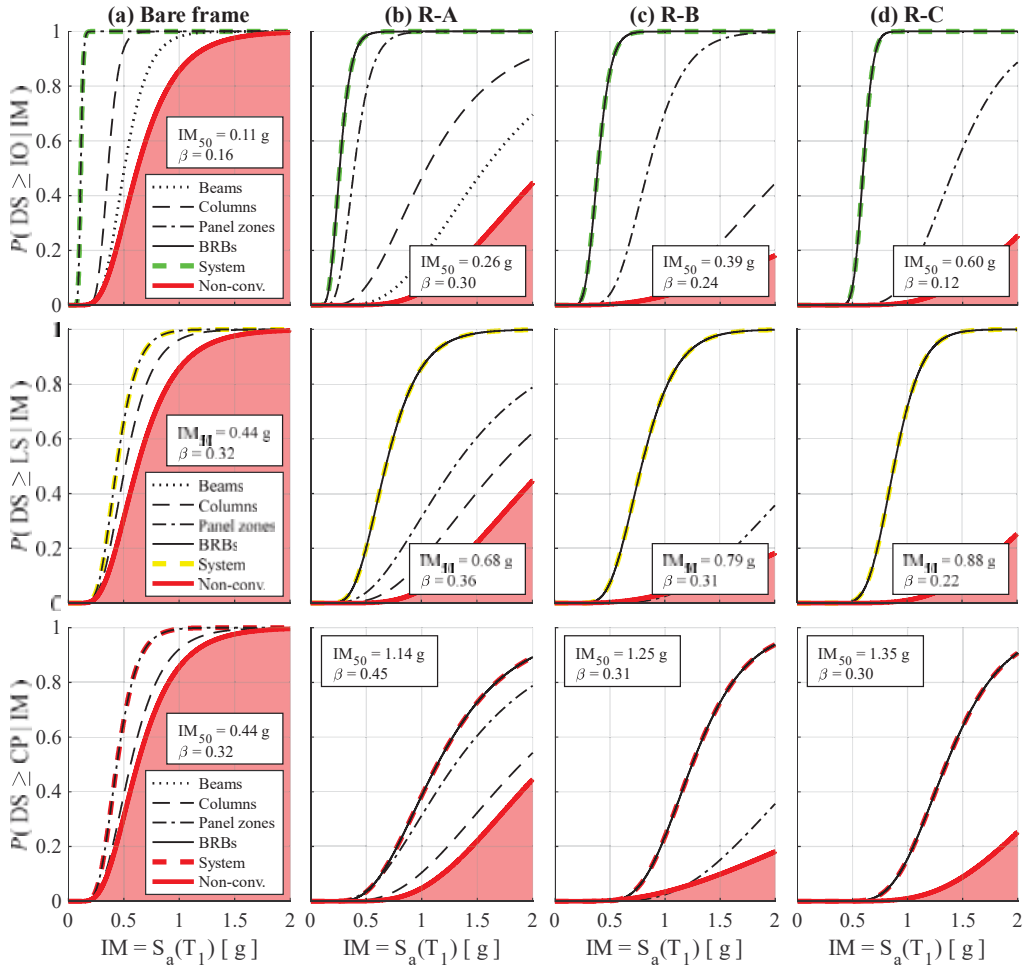

Figure 6: Element-based fragility curves for the IO, LS and CP PLs. The parameters IM_{50} and β are shown for each system fragility curve.

Finally, for comparison purposes only, Figure 7 shows the fragility curves for the monitored global EDPs, which include the Peak Inter-storey Drift Ratios (PIDRs), the Residual Inter-storey Drift Ratios (RIDRs) and Peak Storey Accelerations (PSAs). The AC thresholds for the PIDR of 0.5%, 1.5%, and 2%, suggested by the ASCE 41-06 [31] for braced frames, respectively for IO, LS and CP PLs have been assumed in this study. For the RIDR, an AC thresholds of 0.5% is used, in accordance with McCormick *et al.* [9], which was defined with the aim of controlling building repairability. Finally, the AC thresholds for PSA have been assumed based on the limits used by the Hazus-MH MR4 Technical Manual [32] for moderate-code structures, corresponding to 0.5g, 1.0g and 2.0g for the Moderate, Extensive and Complete PLs.

As shown in Figure 7, the median (*i.e.,* IM_{50}) values for the PIDR and the RIDR fragility curves are increased as the stiffness of the structure is increased, as expected. In the case of the IM_{50} for the PSA fragility curves, all the retrofitting schemes exhibit similar values for the first two thresholds (*i.e.,* 0.5g, 1.0g); however, when the largest acceleration threshold (*i.e.,* 2.0g) is considered, the stiffest structures exhibit larger IM_{50} values. Similarly to the element-based fragility curves, the β parameter is larger in the retrofitting schemes with larger ductility in the BRBF. Also, the dispersion is observed to be larger for the RIDR and PSA fragility curves.

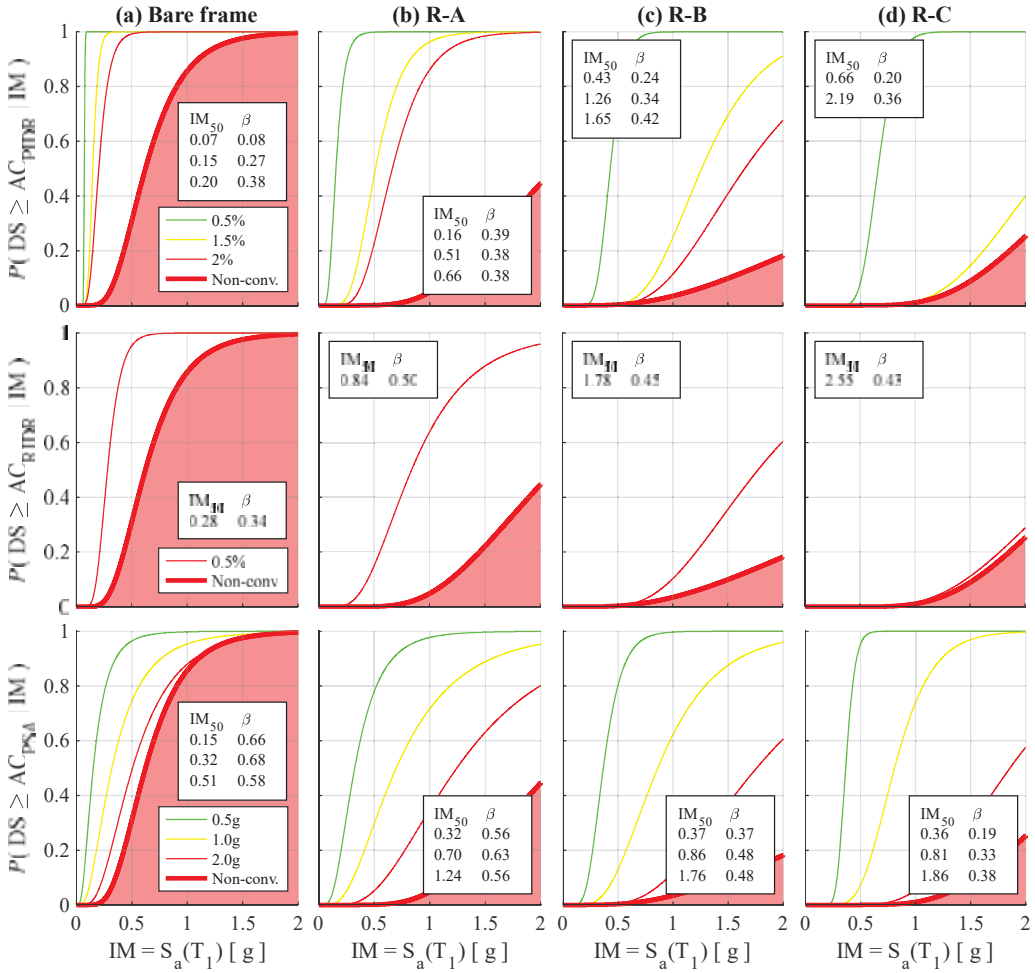

Figure 7: Global fragility curves for the peak inter-storey drift ratios -PIDR- (top), residual inter-storey drift ratios -RIDR- (middle) and peak storey accelerations -PSA- (bottom), for different performance limits (PLs).

4 CONCLUSIONS

This paper presented the fragility assessment of a case-study steel Moment Resisting Frame (MRF) retrofitted with Buckling Restrained Braces (BRBs). Three retrofit configurations were considered which aimed at achieving different performance levels (PLs): R-A was designed to protect the MRF elements from reaching the Collapse Prevention (CP) Performance Limit (PL); R-B was designed to avoid a Peak Inter-storey Drift Ratio larger than 2% at any storey; while R-C was designed to protect the MRF elements from reaching the Immediate Occupancy (IO) PL. The assessment of the bare frame and of the three retrofitting solutions was carried out both by pushover analyses and by Incremental Dynamic Analyses (IDAs). IDAs were performed by using a set of 30 Ground Motion (GM) records, and fragility curves were successively derived by considering limits for element-based and global Engineering Demand Parameters (EDPs).

The following conclusions can be drawn:

- The R-A fragility was controlled by the BRBs in all PLs, closely followed by the panel zones in the IO and CP PLs. In the R-B scheme, the BRBs were capable of protecting the MRF from damage (*i.e.*, overpassing the IO PL) up to a Life Safety (LS) PL in the BRBs. Finally, the R-C scheme was capable of protecting the MRF from damage up to a CP PL, as originally intended during the retrofitting design. These observations are made based on both the non-linear static and the fragility assessments.
- In the case of the global EDPs, the retrofitted structures exhibited a lower probability of exceeding the PLs for all the values of intensity measure (IM), when compared to the bare frame. The stiffer retrofitting schemes were capable of reducing the Peak and Residual Inter-storey Drift Ratios (PIDR and RIDR) for all the values of IM. Conversely, for Peak Storey Acceleration (PSA), the fragility curves derived by considering low acceleration limits (*e.g.*, 0.5g and 1.0g) is similar for all retrofitting schemes. For larger limits of acceleration (*e.g.*, 2.0g), the probability of exceedance is reduced for all values of IM in the stiffer retrofitting schemes (*i.e.*, R-B and R-C).
- In all fragility curves, the dispersion of the distribution (represented by the lognormal standard deviation, β) is increased in structures with larger ductility (*e.g.*, R-A) while it is reduced in structures with lower ductility (*e.g.*, R-C). In all cases, the fragility curves for the RIDR and the PSA exhibit larger β values, in comparison to other EDPs. This is consistent with other studies present in the literature.
- Despite the increase of axial demands in the column and beam elements due to the trussing effects provided by the braces, none of the retrofitting schemes exhibited force-controlled failures in these elements earlier than any of the deformation-controlled acceptance criteria (AC) defined.
- In general, the median capacity (represented by IM_{50}) of the retrofitted structures was benefited from larger retrofitting options, in particular, when large PLs are considered as limits (*e.g.*, CP). The dispersion of the fragility distribution (β) generally increased when considering higher PLs, as well as when considering the RIDR and PSA in comparison with other EDPs. In addition, larger values of β were observed when the Buckling Restrained Braced Frames (BRBFs) within the dual systems were designed for larger ductility targets (*e.g.* R-A).

It is noteworthy that the comparison in terms of fragility only does not provide information on the retrofit's effectiveness, as it considers the variation of the capacity alone. Future work is required toward the inclusions of considerations related to the seismic demand variation for the different retrofit options (*e.g.,* risk definition).

REFERENCES

[1] F.M. Mazzolani, G. Della Corte, M. D'Aniello, Experimental analysis of steel dissipative bracing systems for seismic upgrading, J. Civ. Eng. Manag. 15 (2009) 7–19. https://doi.org/10.3846/1392-3730.2009.15.7-19.

[2] F. Freddi, E. Tubaldi, L. Ragni, A. Dall'Asta, Probabilistic performance assessment of low-ductility reinforced concrete frames retrofitted with dissipative braces, Earthq. Eng. Struct. Dyn. 42 (2013) 993–1011. https://doi.org/10.1002/eqe.2255.

[3] L. Di Sarno, G. Manfredi, Seismic retrofitting with buckling restrained braces: Application to an existing non-ductile RC framed building, Soil Dyn. Earthq. Eng. 30 (2010) 1279–1297. https://doi.org/10.1016/j.soildyn.2010.06.001.

[4] F. Freddi, E. Tubaldi, A. Zona, A. Dall'Asta, Seismic performance of dual systems coupling moment-resisting and buckling-restrained braced frames, Earthq. Eng. Struct. Dyn. (2020) 1–25. https://doi.org/10.1002/eqe.3332.

[5] A. Zona, A. Dall'Asta, Elastoplastic model for steel buckling-restrained braces, J. Constr. Steel Res. 68 (2012) 118–125. https://doi.org/10.1016/j.jcsr.2011.07.017.

[6] T.T. Soong, B.F. Spencer, Supplemental energy dissipation: State-of-the-art and state-of-the-practice, Eng. Struct. 24 (2002) 243–259. https://doi.org/10.1016/S0141-0296(01)00092-X.

[7] R. Tremblay, L. Poncet, P. Bolduc, R. Neville, R. DeVall, Testing and design of buckling restrained braces for canadian application, 13th World Conf. Earthq. Eng. (2004).

[8] J. Erochko, C. Christopoulos, R. Tremblay, H. Choi, Residual Drift Response of SMRFs and BRB Frames in Steel Buildings Designed according to ASCE 7-05, J. Struct. Eng. 137 (2011) 589–599. https://doi.org/10.1061/(asce)st.1943-541x.0000296.

[9] J. McCormick, H. Aburano, M. Ikenaga, M. Nakashima, Permissible Residual Deformation Levels for Building Structures Considering both Safety and Human Elements, 14th World Conf. Earthq. Eng. (2008) 8.

[10] Y. Iwata, H. Sugimoto, H. Kuwamura, Reparability limit of steel structural builidings : Study on performance based design of steel structural buildings, Part 2, J. Struct. Constr. Eng. 70 (2005) 165–172. https://doi.org/10.3130/aijs.70.165_1.

[11] E. Elettore, F. Freddi, M. Latour, G. Rizzano, Design and analysis of a seismic resilient steel moment resisting frame equipped with damage-free self-centering column bases, J. Constr. Steel Res. 179 (2021) 106543. https://doi.org/10.1016/j.jcsr.2021.106543.

[12] F. Morfuni, F. Freddi, C. Galasso, Seismic performance of dual systems with BRBs under mainshock-aftershock sequences, 13th Int. Conf. Appl. Stat. Probab. Civ. Eng. ICASP 2019. (2019) 1–8.

[13] H. Choi, J. Erochko, C. Christopoulos, R. Tremblay, Comparison of the seismic response of steel buildings incorporating self-centering energy-dissipative braces, buckling restrained braces and moment-resisting frames, Res. Rep. 05-2008. (2008).

[14] American Society of Civil Engineers, Seismic Evaluation and Retrofit of Existing Buildings, ASCE/SEI 41-17. (2017). https://doi.org/10.1061/9780784414859.

[15] D. Vamvatsikos, C. Allin Cornell, Incremental dynamic analysis, Earthq. Eng. Struct.

Dyn. 31 (2002) 491–514. https://doi.org/10.1002/eqe.141.

[16] A. Gupta, H. Krawinkler, Behavior of Ductile SMRFs at Various Seismic Hazard Levels, J. Struct. Eng. 126 (2000) 98–107.

[17] G. Teng, J. Baker, Evaluation of SCEC cybershake ground motions for engineering practice, Earthq. Spectra. 35 (2019) 1311–1328. https://doi.org/10.1193/100918EQS230M.

[18] F. McKenna, G.L. Fenves, M.H. Scott, Open system for earthquake engineering simulation (OpenSees), (2000).

[19] F. Gutiérrez-Urzúa, F. Freddi, L. Di Sarno, Comparative analysis of code-based approaches for seismic assessment of existing steel moment resisting frames, J. Constr. Steel Res. 181 (2021) 106589. https://doi.org/10.1016/j.jcsr.2021.106589.

[20] American Institute of Steel Construction, Seismic Provisions for Structural Steel Buildings, 2016. https://doi.org/10.1201/b11248-8.

[21] F. Freddi, C.A. Dimopoulos, T.L. Karavasilis, Experimental Evaluation of a Rocking Damage-Free Steel Column Base with Friction Devices, J. Struct. Eng. 146 (2020) 04020217. https://doi.org/10.1061/(asce)st.1943-541x.0002779.

[22] M. Latour, M. D'Aniello, M. Zimbru, G. Rizzano, V. Piluso, R. Landolfo, Removable friction dampers for low-damage steel beam-to-column joints, Soil Dyn. Earthq. Eng. 115 (2018) 66–81. https://doi.org/10.1016/j.soildyn.2018.08.002.

[23] P. Fajfar, A Nonlinear Analysis Method for Performance-Based Seismic Design, Earthq. Spectra. 16 (2000) 573–592. https://doi.org/10.1193/1.1586128.

[24] Structural Engineers Association of California (SEAOC), California's Office of Statewide Health Planning and Development (OSHPD), U.S. Seismic Design Maps, (2020). https://seismicmaps.org.

[25] American Society of Civil Engineers, Minimum Design Loads and Associated Criteria for Buildings and Other Structures, ASCE/SEI 7-16. (2017). https://doi.org/10.1061/9780784414248.

[26] F. Freddi, J. Ghosh, N. Kotoky, M. Raghunandan, Device Uncertainty Propagation in Low-Ductility RC Frames Retrofitted with BRBs for Seismic Risk Mitigation, Earthq. Eng. Struct. Dyn. (2021). https://doi.org/10.1002/eqe.3456.

[27] L.A. Fahnestock, R. Sause, J.M. Ricles, L.-W. Lu, Ductility demands on buckling-restrained braced frames under earthquake loading, Earthq. Eng. Eng. Vib. 2 (2003) 255–268. https://doi.org/10.1007/s11803-003-0009-5.

[28] Y. Bozorgnia, N.A. Abrahamson, L. Al Atik, T.D. Ancheta, G.M. Atkinson, J.W. Baker, A. Baltay, D.M. Boore, K.W. Campbell, B.S.-J. Chiou, R. Darragh, S. Day, J. Donahue, R.W. Graves, N. Gregor, T. Hanks, I.M. Idriss, R. Kamai, T. Kishida, A. Kottke, S.A. Mahin, S. Rezaeian, B. Rowshandel, E. Seyhan, S. Shahi, T. Shantz, W. Silva, P. Spudich, J.P. Stewart, J. Watson-Lamprey, K. Wooddell, R. Youngs, NGA-West2 Research Project, Earthq. Spectra. 30 (2014) 973–987. https://doi.org/10.1193/072113EQS209M.

[29] F. Freddi, J.E. Padgett, A. Dall'Asta, Probabilistic seismic demand modeling of local level response parameters of an RC frame, Bull. Earthq. Eng. 15 (2017). https://doi.org/10.1007/s10518-016-9948-x.

[30] F. Jalayer, H. Ebrahimian, A. Miano, G. Manfredi, H. Sezen, Analytical fragility assessment using unscaled ground motion records, Earthq. Eng. Struct. Dyn. 46 (2017) 2639–2663. https://doi.org/10.1002/eqe.2922.

[31] American Society of Civil Engineers, Seismic Rehabilitation of Existing Buildings, ASCE/SEI 41-06. (2007). https://doi.org/10.1061/9780784408841.

[32] Federal Emergency Management Agency, HAZUS-MH MR4 Technical Manual, Natl. Inst. Build. Sci. Fed. Emerg. Manag. Agency (NIBS FEMA). (2003) 712.